Med Bio Eng Comput (2006) 44:583–591
DOI 10.1007/s11517-006-0067-8

ORIGINAL ARTICLE

An investigation of the use of transmission ultrasound to measure acoustic attenuation changes in thermal therapy

Neeta Parmar · Michael C. Kolios

Received: 29 January 2006 / Accepted: 20 April 2006 / Published online: 10 June 2006

Abstract The potential of using a commercial ultrasound transmission imaging system to quantitatively monitor tissue attenuation changes after thermal therapy was investigated. The ultrasound transmission imaging system used, the AcoustoCam (Imperium Inc., MD) allows ultrasonic images to be captured using principles similar to that of a CCD-type camera that collects light. Ultrasound energy is focused onto a piezoelectric array by an acoustic lens system, creating a gray scale acoustic image. In this work, the pixel values from the acoustic images were assigned acoustic attenuation values by imaging polyacrylamide phantoms of varying known attenuation. After the calibration procedure, data from heated polyacrylamide/bovine serum albumin (BSA) based tissue-mimicking (TM) phantoms and porcine livers were acquired. Samples were heated in water at temperatures of 35, 45, 55, 65, and 75°C for 1 h. Regions of interest were chosen in the images and acoustic attenuation values before and after heating were compared. An increase in ultrasound attenuation was found in phantoms containing BSA and in porcine liver. In the presence of BSA, attenuation in the TM phantom increased by a factor of 1.5, while without BSA no significant changes were observed. The attenuation of the porcine liver increased by up to a factor of 2.4, consistent with previously reported studies. The study demonstrates the feasibility of using a quantitative ultrasound transmission imaging system for monitoring thermal therapy.

Keywords Thermal therapy · Acoustic attenuation · Ultrasound phantoms · Gel attenuation · Ultrasound attenuation mapping

N. Parmar · M. C. Kolios
Department of Electrical and Computer Engineering,
Ryerson University, 350 Victoria Street,
Toronto, ON, Canada M5B-2K3

M. C. Kolios (✉)
Department of Physics, Ryerson University,
350 Victoria Street, Toronto, ON, Canada M5B-2K3
e-mail: mkolios@ryerson.ca
URL: http://www.physics.ryerson.ca

1 Introduction

Thermal therapy is an attractive alternative to surgery and radiation therapy because of its ability to locally kill tumors while preserving surrounding normal tissues [27]. The target tissue is heated to high temperatures (between 50 and 100°C), leading to rapid destruction. An integral part of the success of thermal therapy is a real-time monitoring system to monitor tissue damage in order to control the area being heated and protects the surrounding normal tissue. Ultrasound (US) monitoring may be useful since it is non-invasive and it can be done in real-time. Several groups have investigated the change in acoustic properties of heated tissue, showing that tissue ultrasound attenuation rises for temperatures above 55°C. Worthington and Sherar [31] investigated changes in ultrasound backscatter and attenuation for 30 min exposure times at temperatures up to 65°C in porcine kidney. They found an increase in attenuation of a factor of ~1.9 after 30 min. Clarke et al. [3] and Gertner et al. [6] measured attenuation changes for higher temperature heating protocols (70–80°C) and found attenuation increases of up to 2.4 dB/cm. These studies show that

depending on tissue type, temperature, and heating time, attenuation can increase by a factor of 3.5 and recent data indicate up to a factor of seven for temperatures above 80°C [29]. Therefore, attenuation seems to be the most robust parameter for ultrasound-based monitoring of thermal therapies. These studies indicate that a method of measuring tissue attenuation can be useful for monitoring thermal therapy; but knowing how attenuation changes with treatment is also critical for modeling ultrasonic treatments [14, 29].

This paper investigates the potential of using real-time ultrasound transmission imaging to monitor ultrasound attenuation changes. Magnetic resonance imaging (MRI) [9, 26, 30], US [1, 17] and computed tomography (CT) [2, 8] have all been investigated to monitor thermal therapy, however these methods are either expensive, lack accurate real-time monitoring, have poor contrast or temporal resolution. Transmission ultrasound is an alternative to previously studied methods of monitoring thermal therapy. It directly measures tissue attenuation, which is known to significantly change upon tissue coagulation. King et al. [13] investigated the use of transmission ultrasound imaging, using a similar system to that used in this study. Using high-intensity focused US to heat tissues they were able to observe reversible time-dependant variations in transmission ultrasound images in bovine fat, rabbit liver, and porcine liver. These data demonstrate the potential of using transmission ultrasound in monitoring tissue damage, however the results were presented in terms of pixel values obtained from the camera's images, and a quantitative change in attenuation was not presented. It was therefore not possible to gage the sensitivity of the technique to the attenuation changes expected in clinical situations. In this paper, calibration experiments are presented that allow the direct correlation of the pixel intensity to ultrasound attenuation. Phantoms with variable known attenuation values are made and imaged. A temperature sensitive agent is added to the phantoms to examine how it would influence the phantom attenuation. Finally, excised porcine liver is heated to different temperatures to demonstrate the technique applicability in tissues.

2 Materials and methods

2.1 The AcoustoCam system

An ultrasound transmission camera, developed by Imperium Inc. (Rockville, MD) was used in this study. The system, called the AcoustoCam, uses a 5 MHz unfocused planar transducer to illuminate the target tissue. The resultant pressure wave strikes the tissue and is scattered and attenuated. The transmitted ultrasound energy is focused onto a piezoelectric array by an acoustic lens system (Fig. 1). The lens system consists of a pair of acoustic lenses. The outermost lens is in a fixed position, while the innermost lens is moveable (using a focusing knob) to achieve good focus. The piezoelectric array is 1 cm^2 with 120×120-pixel elements and 0.083 mm pixel spacing. The ultrasound energy that strikes the array is converted to an analog voltage, which is digitized and fed into a frame grabber (Matrox Meteor II), which is installed on a PC [15, 16]. Images are recorded via a RS-170 video stream at a rate of 30 frames/s. Real-time imaging and still image recording was done using the Acoustocam imaging software, and image processing was done using Matlab® (Mathworks, Inc.). The images recorded through the camera's software are gray-scale images, resulting in pixel values ranging from 0 to 255. The lower the pixel value, the darker it appears in the image. A low pixel value is observed when little ultrasound energy is captured by the array. Hence, objects imaged with high ultrasound attenuation properties will result in darker images.

The control unit of the system, which sends excitation pulses using a spike pulser, controls the transducer. The pulser sends a 4.3 MHz impulse with a user-adjustable peak voltage ranging from 240 to 1,000 V to the transducer. Within the Acoustocam software, the capture window width and transducer distance settings are set to match the physical distance between the transducer and array. The capture window width is the amount of time the camera detector is turned on. The higher the value, the more of the incident ultrasound energy will be integrated to form the image. The transducer distance is the length of water path from the transducer to the array, and is based on the assumption of an ultrasound velocity of 1,500 m/s. The capture window width and the transducer signal are synchronized through the transducer distance, which compensates for the time it takes the ultrasound pulse to travel through water. This distance can be changed depending on the speed of sound of the object being imaged.

2.2 Sample preparation

A tissue-mimicking (TM) phantom based on the recipe developed by McDonald et al. [21] was used. The phantom consists of a polyacrylamide gel mixed with bovine serum albumin (BSA). BSA is a temperature sensitive protein that undergoes thermal denaturation

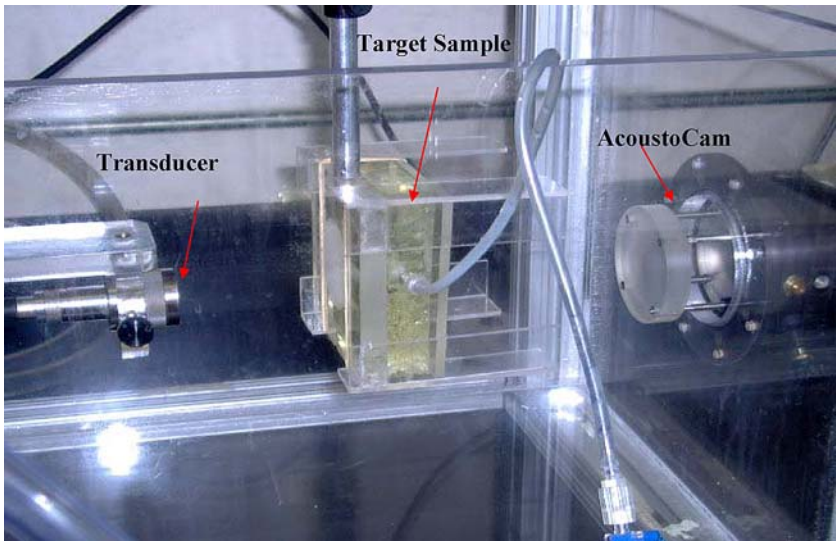

Fig. 1 Photograph of the experimental setup showing the positions of the transducer, target to be imaged and the AcoustoCam

and assists in the visualization of the coagulated region [11 12]. Exposure to heat causes an unfolding of the bovine albumin proteins, which then precipitate out of solution and rapidly form albumen aggregates. Translucent phantoms visibly whiten during this process. This can be quantified by an increase in the reduced scattering coefficient [22]. The polyacrylamide gel was used because of its stability at high temperatures, as opposed to other gels (such as gelatin or agar), which have lower melting temperatures. To verify the role of BSA and the stability of the polyacrylamide gel, phantoms were produced with and without BSA and heating experiments were conducted on such phantoms. A complete recipe and detailed instructions for constructing the phantom is provided by McDonald et al. [21].

Adding different concentrations of Intralipid® to the phantom recipe modifies the ultrasound absorption properties of the phantom. Phantoms of varying attenuation were used for camera calibration. This was achieved by making phantoms with different thicknesses and different attenuation coefficients (Table 1). These phantoms were used in the calibration experiments. On the other hand, for all phantom heating experiments no Intralipid® was used, resulting in an attenuation coefficient of 0.26 ± 0.02 dB cm^{-1} MHz^{-1}, and speed of sound 1548 ± 4 ms^{-1} [21]. Porcine liver tissue used in the study was purchased from a local grocery store. Samples remained sealed in its packaging until it was ready to be used to avoid gassing of the liver, and were used no longer than a few hours after purchase.

2.3 Experimental setup

Experiments were conducted in a tank filled with degassed and deionized water. Echowet® (Sonotech Inc., Bellingham, WA) was added to the tank, an immersion additive that lowers the surface tension of the water, thereby releasing air bubbles, which may otherwise interfere with the ultrasound waves. The transducer was placed 30.5 cm from the camera, and the samples were placed approximately in the middle of the two. A photograph of the experimental setup is shown in Fig. 1.

2.4 AcoustoCam calibration procedure

Images obtained from the AcoustoCam were quantified in terms of attenuation values by calibrating the instrument. The AcoustoCam system has a ‘dynamic

Table 1 Acoustic attenuation for phantoms with added Intralipid® concentrations

Phantom	Attenuation coefficient (dB cm^{-1} MHz^{-1})	Thickness (cm)	Attenuation @ 5 MHz (dB)
TM phantom, no Intralipid	0.26	2.5	3.25
TM phantom, 15% Intralipid® (v/v)	0.35	2.2 and 3.3	3.85 and 5.78
TM phantom, 30% Intralipid® (v/v)	0.52	2.0 and 3.5	5.2 and 9.1
TM phantom, 45% Intralipid® (v/v)	0.67	2.0 and 4.0	6.5 and 13.0
TM phantom, 60% Intralipid® (v/v)	0.78	3.0, 4.3, 5.5 and 7.7	11.55, 16.56, 21.18 and 29.65

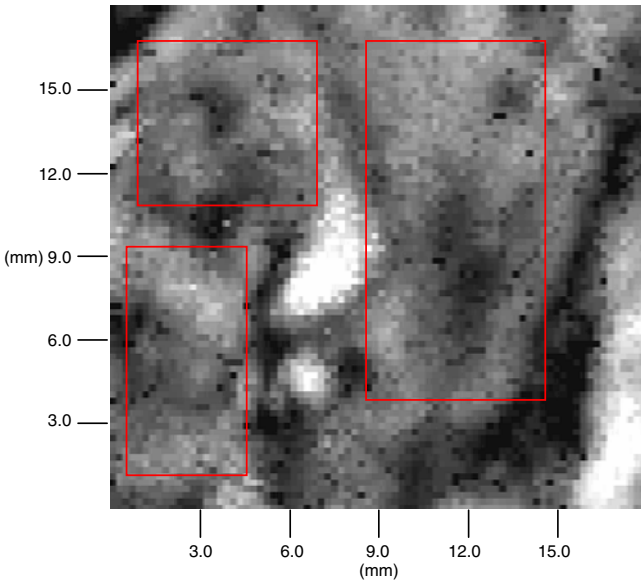

Fig. 2 Example of ROI selection for porcine liver images. In the image ROIs were selected in areas to avoid occasional large non-uniformities

range correction' feature in which the digital values can be re-mapped for a desired grey-scale range. This re-mapping is accomplished by truncating the upper and lower ranges of the 14-bit (16,383 levels) digital values for presentation within the 8-bit (256 levels) display. The dynamic range was optimized for an attenuation range of 0–21 dB by imaging various samples with known attenuation within this range, and adjusting the upper and lower ranges of the 14-bit digital values. Phantoms with varying Intralipid® concentration and thickness were constructed and imaged to extract the relation between pixel values and acoustic attenuation. Attenuation values of the phantoms with variable attenuation are listed in Table 1, following the recipe from McDonald et al. [21]. The mean pixel intensity value versus attenuation data was curve fit to a third-order polynomial. This polynomial expression represents the relation between the grey scale image pixel intensity and attenuation in dB and was used in other experiments to relate the observed pixel values to acoustic attenuation.

2.5 Heating procedure

For each phantom type and liver, 15 samples were used. Each sample was sealed in plastic and immersed in a continuously stirred water-bath preheated and maintained for 1 h at 35, 45, 55, 65, and 75°C. For each temperature experiments were repeated three times on different phantoms/livers of the same sample-type. Phantoms were 10×10×2.5 cm, and liver samples were approximately 10×5×1 cm. The sample was heated for 1 h to ensure that it thoroughly reached a steady state temperature, resulting in uniform temperature throughout the sample. A thermocouple inserted into the center of the sample was used to assure that the sample had reached the desired temperature.

2.6 Data acquisition and analysis

Images recorded through the AcoustoCam software were analyzed using Matlab. Images are displayed in real-time at a rate of 30 frames/s, and stored at a rate of 6 frames/s (depending on the speed of the computer). Due to the large number of images stored, every 24 images were averaged, and the averaged image was used in the analysis. This resulted in an analysis of one averaged image for every 4 s.

For the heating experiments of the phantoms, the mean pixel value was calculated by averaging the pixel values of a region of interest (ROI). Since images of the liver samples contained inhomogenieties in the image, one ROI could not be selected for the entire image. Instead three large ROIs were selected avoiding the large non-uniformities in their presence. Figure 2 gives an example of the ROIs selected in a liver image in the presence of a non-uniformity. Images numbered 500 were taken of each sample before it was placed in the water bath for heating. After 1 h of heating at the desired temperature, the sample was then placed into the sample holder and back into the imaging tank. Images were taken for 10 min while the sample cooled to 22°C (ambient temperature of the tank water). Temperatures were recorded while the sample cooled using an Omega data-logger thermometer (OMEGA-ETTE HH306 series).

3 Results

Figure 3a presents the AcoustoCam images for phantoms with varying attenuation. Mean image pixel values of each phantom were plotted against the phantom attenuation, and this plot was fit to a third-order polynomial, shown in Fig. 3b. The camera calibration procedure confirmed the camera's capabilities for measuring varying attenuation. The camera dynamic range was adjusted to image a limited range of 0–21 dB (instead of 60 dB, the default setting), resulting in increased camera sensitivity to smaller changes in ultrasound attenuation. The calibration curve of Fig. 3b was used in subsequent experiments. More details can be found elsewhere [23].

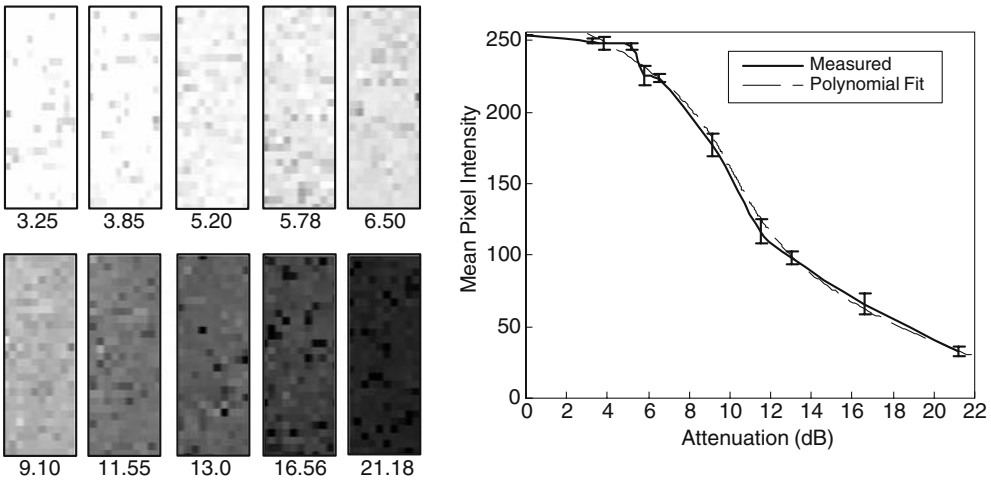

Fig. 3 **a** Cropped acoustic images of various phantoms with different acoustic attenuation. The value below each image is the attenuation of the phantom in dB. **b** Pixel value response of the camera. The *faded line* is the result of the polynomial curve fit used to map attenuation values in future experiments. *Error bars* represent deviation between the 20 consecutive regions selected across the entire image as a measure of phantom uniformity

AcoustoCam images of an unheated phantom compared to heated phantoms at 35, 45, 55, 65, and 75°C for phantoms containing BSA are shown in Fig. 4a. Images are of heated phantoms after 10 min of cooling, at which point the sample reached ambient temperature (22°C, verified by thermocouple measurement). The attenuation of an unheated sample was 1.45±0.16 dB cm^{-1}. The normalized change in attenuation between the unheated and heated samples after reaching room temperature was calculated by

$$\alpha_{\text{normalized}} = \frac{\alpha_{\text{heated}}}{\alpha_{\text{unheated}}}$$

Results shown in Fig. 4c indicate an increase in attenuation with temperature after 1 h of heating. The normalized change in attenuation ranged from 1.02 to 1.42 for temperatures from 35 to 75°C for the phantoms with the BSA.

As seen in the acoustic images of the heated phantoms with no BSA (Fig. 4b), there was little change in acoustic properties with temperature. Moreover, the standard deviation of the sample measurement was small, indicating better sample uniformity compared to the phantoms exposed to different temperatures. Samples also did not turn opaque for any heating temperature exposure due to the lack of BSA, while samples with BSA were less translucent. Figure 4c shows the normalized change in attenuation measured after the sample was cooled to ambient temperature.

Figure 5a presents acoustic images of heated liver at different temperature exposures. The attenuation of unheated liver was 4.01±0.23 dB cm^{-1}. Image darkening was observed with increasing temperature, greater than that observed in the phantoms, indicating a larger increase in attenuation. The normalized change in liver attenuation is shown in Fig. 5b. There is a gradual increase in the liver attenuation, with the largest relative change in attenuation occurring at 75°C.

4 Discussion

Results in this study show that the AcoustoCam is sensitive to changes in ultrasound attenuation induced by heating in phantoms and porcine liver. Significant darkening was observed in the acoustic images, corresponding to an increase in ultrasound attenuation. The system was calibrated so that quantitative changes in the sample attenuation could be measured. Depending on the dynamic range chosen, relatively small changes in overall attenuation could be measured (Fig. 3b), indicating that the technique could be used for thermal therapy monitoring. For typical thermal lesions, 1–2 cm in diameter, the attenuation contrast is expected to be several dB, and thus readily detectable with the current system. In should be noted that the calibration values presented are specific to the camera and detector chip, therefore the method would have to be repeated for each instrument used.

Figure 4c shows a plot of acoustic attenuation as a function of temperature for the phantoms with and without BSA. Changes observed in phantoms with BSA as opposed to those without indicate that the presence of BSA denaturation changes both the optical and acoustical properties of the phantom. Howard et al. [10] also studied acoustic attenuation changes in a polyacrylamide-BSA based phantom, and found an increase in attenuation with temperatures up to 60°C. The amount of BSA included in the phantom can be controlled, so that specific phantoms could be made to emulate overall changes in attenuation for specific tissues. Interesting parallels can be drawn from the field of radiation dosimetry. In studies

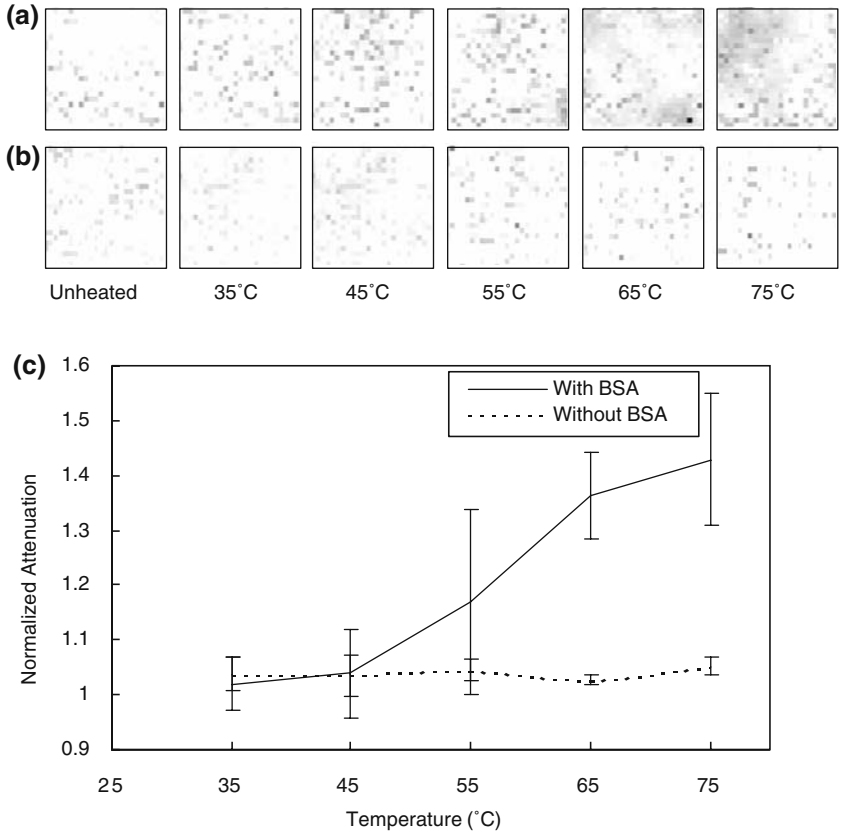

Fig. 4 **a** Acoustic images for phantoms containing BSA heated at various temperatures. **b** Acoustic images for phantoms not containing BSA heated at various temperatures. All images are 2.0×2.0 mm. **c** Normalized attenuation changes as a function of temperature (normalized to room temperature). *Error bars* represent the standard deviation of three experiments

of gels for radiation dose calculation based on ultrasound attenuation, Mather et al. [18–20] concluded that relaxation mechanisms contribute to absorption in polymer gel dosimeters, and that the mechanisms involved are likely to be solute–solvent interactions and motion of polymer side chain groups. They have proposed that acoustic transmission measurements could also thus be utilized for radiation dosimetry, as the sensitivity of the gels they have developed is 4.7±0.3 dB m^{-1} Gy^{-1}. Future work may involve developing such measurement as a function of thermal dose for thermal therapies.

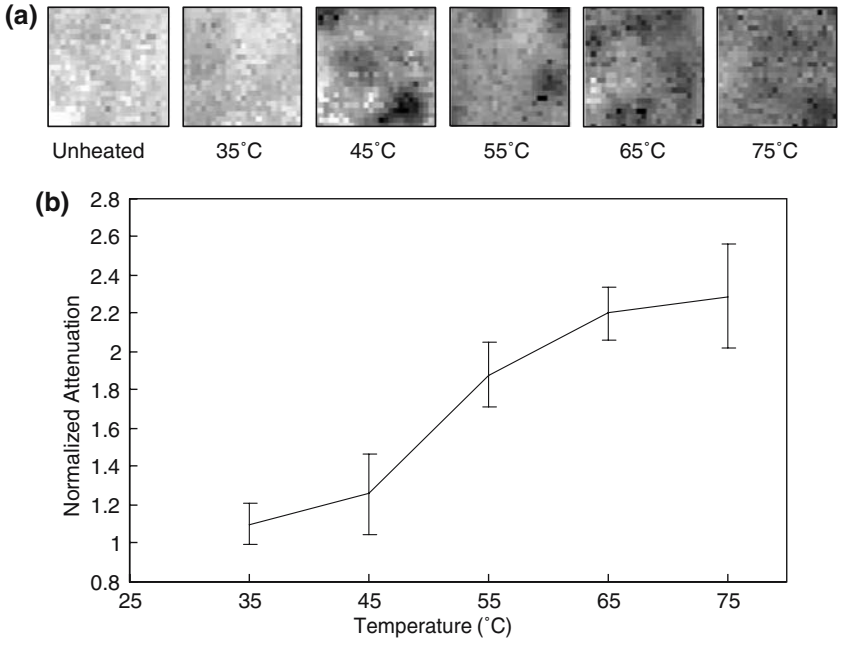

Fig. 5 **a** Acoustic images for liver samples heated at various temperatures. All images are 2.0×2.0 mm. **b** Normalized attenuation changes as a function of temperature (normalized to room temperature). *Error bars* represent standard deviation of three experiments

Coagulation was visible in phantoms containing BSA. The change in opaqueness with temperature is due to the BSA denaturation therefore it was hypothesized that if the phantom did not have BSA there would be no change in both the optical and acoustic properties of the heated phantom. Figure 4c shows little acoustic change in the TM phantom without BSA as a function of temperature. This indicates that BSA is a temperature-sensitive marker and furthermore that the polyacrylamide phantoms are resistant to the temperature-time exposures of this study. The change in acoustic properties with BSA content could thus be used to model dynamic acoustic changes in tissue properties during ultrasound heating, akin to studies done for laser thermal therapies [12], important for computational model validation.

Little change was observed in the attenuation coefficient of the porcine liver for the exposures at temperatures below 45°C. A general increase in attenuation coefficient with temperature was observed at 45°C and greater. This agrees with previously reported studies on bovine liver [6, 31], canine liver [5], and porcine kidney [4]. Gertner et al. [6 7 showed an increase by a factor 1.85 over 30 min of heating at 70°C. In this study, we observed a factor increase of 2.29 at 60 min of heating at 75°C. At 65°C Gertner et al. [6] observed an increase of a factor of 1.4, and we observed an increase of 2.2. Attenuation results from Gertner et al. [6] were made at the elevated temperature, whereas results presented in this study are after the sample has cooled. Techavipoo et al. [28] found that when attenuation was measured for coagulated tissue at the elevated temperature, no significant change in ultrasonic attenuation could be detected, but when the attenuation of the tissue was measured at ambient temperature the increase in attenuation could be readily measured. Temperature elevation and coagulation appear to have opposite effects on attenuation, an important consideration to take into account when modeling the process, especially in light of recent data that show for temperatures greater than 80–90°C attenuation increases of a factor of seven for chicken breast tissue [29]. For water and at 5 MHz, the attenuation drops from 0.55 to 0.15 dB cm^{-1} at 90°C [25]. As water is a major constituent of tissue, a similar effect can be hypothesized. Such results indicate that monitoring attenuation changes during thermal therapy with elevated temperatures is difficult since the temperature dependence of attenuation decreases the measured attenuation, while the structural changes in coagulated tissue increase the measured attenuation. For the temperatures achieved during thermal therapies these effects are similar in magnitude for liver and likely other tissues. However, after heating it is hypothesized that lesions will be visible using transmission ultrasound as there is an increase in tissue attenuation. Moreover, if during heating, vaporization occurs due to the high temperatures reached, the effective attenuation increases significantly and this should be visible by the acoustic camera [23].

The ultrasound attenuation data obtained by the calibrated acoustic camera also agree with literature values. Techavipoo et al. [28] found that the attenuation coefficient after heating increased almost linearly up to 6 dB/cm (at 5 MHz) when the target temperature increased from 50 to 90°C. The values are similar to those presented in this study. Techavipoo et al. [28] measured an attenuation of the canine liver at 22°C of 4.01±0.269 dB cm^{-1} (similar to our measurement of 4.01±0.230 dB cm^{-1}), Tyreus and Diederich [29] measured an attenuation of 1.3 dB cm^{-1} for bovine liver at 37°C and Clarke et al. [3] 2 dB cm^{-1} for porcine liver at 37°C. The device has the potential to provide ultrasound attenuation data during a thermal therapy treatment. However, the instrument provides an attenuation value that represents the integrated attenuation over the entire beam path, making it difficult to localize the attenuation increase. Tomographic approaches could be applied to localize the lesion [18]. Moreover, the temperature effect, which locally decreases the tissue attenuation, further complicates the data analysis. We are investigating the potential of the camera to distinguish between the two effects [23, 24]. Monitoring the attenuation changes during heating produces subtle effects due to the tissue and water attenuation temperature dependence.

These pilot experiments show the potential of the acoustic camera for real-time imaging of phantoms and tissues and for thermal lesions that are created. Modifications to the setup would be required if the technique were to be used to image humans. Instead of the current configuration, another model of the camera would be required that would allow direct coupling of the acoustic camera unit to the human body. For example, Imperium Inc. makes a version of the camera, which is handheld and makes direct contact with the object imaged (the AcoustoCam I400 TM Handheld Imager). It could thus be envisioned that depending on the region that is heated, the illuminating transducer is placed at an appropriate location, which would provide a good acoustic window, and the camera unit could be secured in position with a mechanical device or even held in position by hand.

5 Conclusions

It was shown that ultrasound transmission imaging can be used to detect, in a quantitative manner, changes in attenuation that occur as a result of thermal therapy treatments. By optimizing the dynamic range of the instrument, small changes in attenuation could be detected. Temperature dependent increases in attenuation were measured for polyacrylamide-BSA based phantoms, while in the absence of BSA there was no change in attenuation. Porcine liver experiments demonstrated attenuation increases of up to a factor of 2.4 with heating, consistent with other studies.

Acknowledgments This work was supported by funds from the National Sciences and Engineering Research Council of Canada (NSERC), the Canada Foundation for Innovation (CFI), the Ontario Innovation Trust and Ryerson University. The authors thank John Kula and Jack Gurney at Imperium Inc. for their support and Dr. J. Carl Kumaradas for his excellent comments and suggestions. We would also like to thank colleagues, Lenoid Guerchkovitch, Arthur Worthington, and Xia Wu for their technical assistance.

References

1. Bevan PD, Sherar MD (2001) B-scan ultrasound imaging of thermal coagulation in bovine liver: frequency shift attenuation mapping. Ultrasound Med Biol 27(6):809–817
2. Cha CH, Lee FT Jr, Gurney JM, Markhardt BK, Warner TF, Kelcz F, Mahvi DM (2000) CT versus sonography for monitoring radiofrequency ablation in a porcine liver. AJR Am J Roentgenol 175(3):705–711
3. Clarke RL, Bush NL, Ter Haar GR (2003) The changes in acoustic attenuation due to in vitro heating. Ultrasound Med Biol 29(1):127–135
4. Clarke RL, ter Haar GR (1997) Temperature rise recorded during lesion formation by high-intensity focused ultrasound. Ultrasound Med Biol 23(2):299–306
5. Damianou CA, Sanghvi NT, Fry FJ, Maass-Moreno R (1997) Dependence of ultrasonic attenuation and absorption in dog soft tissues on temperature and thermal dose. J Acoust Soc Am 102(1):628–634
6. Gertner MR, Wilson BC, Sherar MD (1997) Ultrasound properties of liver tissue during heating. Ultrasound Med Biol 23(9):1395–1403
7. Gertner MR, Worthington AE, Wilson BC, Sherar MD (1998) Ultrasound imaging of thermal therapy in in vitro liver. Ultrasound Med Biol 24(7):1023–1032
8. Goldberg SN, Kamel IR, Kruskal JB, Reynolds K, Monsky WL, Stuart KE, Ahmed M, Raptopoulos V (2002) Radiofrequency ablation of hepatic tumors: increased tumor destruction with adjuvant liposomal doxorubicin therapy. AJR Am J Roentgenol 179(1):93–101
9. Graham SJ, Chen L, Leitch M, Peters RD, Bronskill MJ, Foster FS, Henkelman RM, Plewes DB (1999) Quantifying tissue damage due to focused ultrasound heating observed by MRI. Magn Reson Med 41(2):321–328
10. Howard S, Yuen J, Wegner P, Zanelli CI (2003) Characterization and FEA simulation for a HIFU phantom material. In: IEEE ultrasonics symposium, pp 1270–1273
11. Iizuka MN, Sherar MD, Vitkin IA (1999) Optical phantom materials for near infrared laser photocoagulation studies. Lasers Surg Med 25(2):159–169
12. Iizuka MN, Vitkin IA, Kolios MC, Sherar MD (2000) The effects of dynamic optical properties during interstitial laser photocoagulation. Phys Med Biol 45(5):1335–1357
13. King RL, Clement GT, Maruvada S, Hynynen K (2003) Preliminary results using ultrasound transmission for image-guided thermal therapy. Ultrasound Med Biol 29(2):293–299
14. Kolios MC, Sherar MD, Hunt JW (1999) Temperature dependent properties and ultrasound thermal therapy. In: Scott EP (ed) Advances in heat and mass transfer in biotechnology HTD-Vol. 363/BED-Vol. 44, ASME international mechanical engineering congress and exposition. American Society of Mechanical Engineers, pp 113–118
15. Lasser M (1997) A novel high speed, high resolution, ultrasound imaging system. In :composites for the real world, pp 179–185
16. Lasser ME, Harrison GH, Agarwal M (1996) Acoustic microscopy for 100% non-destructive semiconductor package evaluation. In: 1996 international symposium on microelectronics, pp 82–86
17. Liu W, Techavipoo U, Varghese T, Zagzebski JA, Chen Q, Lee FT Jr (2004) Elastographic versus x-ray CT imaging of radio frequency ablation coagulations: an in vitro study. Med Phys 31(6):1322–1332
18. Mather ML, Baldock C (2003) Ultrasound tomography imaging of radiation dose distributions in polymer gel dosimeters: preliminary study. Med Phys 30(8):2140–2148
19. Mather ML, Charles PH, Baldock C. 2003a. Measurement of ultrasonic attenuation coefficient in polymer gel dosimeters. Phys Med Biol 48(20):N269–275
20. Mather ML, Collings AF, Bajenov N, Whittaker AK, Baldock C (2003b) Ultrasonic absorption in polymer gel dosimeters. Ultrasonics 41(7):551–559
21. McDonald M, Lochhead S, Chopra R, Bronskill MJ (2004) Multi-modality tissue-mimicking phantom for thermal therapy. Phys Med Biol 49(13):2767–2778
22. Meijerink R, Essepreis M, Pickering J, Massen CH, Mills TN, van Gemert MJC (1995) Rate process parameters of egg white measured by light scattering. In: Muller G, Roggan A, (eds) Laser-induced interstitial thermotherapy. SPIE, p 66
23. Parmar N (2005) An Investigation of using transmission ultrasound to monitor acoustic attenuation changes in thermal therapy. M.Sc. Thesis, Department of Electrical and Computer Engineering, Ryerson University, Toronto, p 88
24. Parmar N, Kolios MC (2004) Attenuation mapping for monitoring thermal therapy using ultrasound transmission imaging. In: 26th annual international conference of the engineering in medicine and biology society, IEEE, p 1329
25. Pinkerton JMM (1949) The absorption of ultrasonic waves in liquids and its relation to molecular constitution. Proc Phys Soc B62:129–141
26. Sherar MD, Moriarty JA, Kolios MC, Chen JC, Peters RD, Ang LC, Hinks RS, Henkelman RM, Bronskill MJ, Kucharcyk W (2000) Comparison of thermal damage calculated using magnetic resonance thermometry, with magnetic resonance imaging post-treatment and histology, after interstitial microwave thermal therapy of rabbit brain. Phys Med Biol 45(12):3563–3576
27. Sherar MD, Trachtenberg J, Davidson SR, Gertner MR (2004) Interstitial microwave thermal therapy and its application to the treatment of recurrent prostate cancer. Int J Hyperthermia 20(7):757–768

28. Techavipoo U, Varghese T, Chen Q, Stiles TA, Zagzebski JA, Frank GR (2004) Temperature dependence of ultrasonic propagation speed and attenuation in excised canine liver tissue measured using transmitted and reflected pulses. J Acoustical Soc Am 115(6):2859–2865
29. Tyreus PD, Diederich C (2004) Two-dimensional acoustic attenuation mapping of high-temperature interstitial ultrasound lesions. Phys Med Biol 49(4):533–546
30. Vitkin IA, Moriarty JA, Peters RD, Kolios MC, Gladman AS, Chen JC, Hinks RS, Hunt JW, Wilson BC, Easty AC, Bronskill MJ, Kucharczyk W, Sherar MD, Henkelman RM (1997) Magnetic resonance imaging of temperature changes during interstitial microwave heating: a phantom study. Med Phys 24(2):269–277
31. Worthington AE, Sherar MD (2001) Changes in ultrasound properties of porcine kidney tissue during heating. Ultrasound Med Biol 27(5):673–682